THE ASTROPHYSICAL JOURNAL, 522:661–668, 1999 September 10

DYNAMICS IN A LOPSIDED SPIRAL GALAXY: NEGATIVE DISK RESPONSE TO PERTURBATION HALO POTENTIAL

CHANDA J. JOG
Department of Physics, Indian Institute of Science, Bangalore 560012, India; cjjog@physics.iisc.ernet.in
Received 1998 July 29; accepted 1999 April 15

ABSTRACT

We study the self-consistent response of an axisymmetric galactic disk perturbed by a constant lopsided ($m = 1$) halo potential and show that the disk self-gravity plays a crucial role in the determination of the net lopsided distribution in the disk. First, the self-gravitational potential corresponding to the nonaxisymmetric density response of the disk to the lopsided potential is calculated, by inversion of the Poisson equation for a thin disk, and this is shown to be negative, that is, it opposes the lopsided halo potential. Next, the net stellar disk response is obtained self-consistently so as to take account of the effect of both the imposed lopsided potential and also the disk response potential. The magnitude of the net lopsided potential in the galactic disk plane is shown to be always smaller than that of the perturbation lopsided potential. The perturbation potential is reduced by a factor that is independent of the strength of the perturbation potential. This factor has a minimum value of ~ 0.5–0.7, which is insensitive to the morphological type and size of the galaxy.

The net lopsided distribution in the disk is shown to be important only beyond a radius of 1.4 disk scale lengths, and its magnitude increases with radius, indicating the increasing dynamical importance of the halo over the disk at larger radii. This is a robust dynamical result and is independent of the logarithmic slope of the rotation curve. This result is in exact agreement with the observations of stellar disks by Rix & Zaritsky (1995). It also provides a natural explanation as to why lopsidedness in the atomic hydrogen gas is observed mainly in the outer disk.

Subject headings: galaxies: halos — galaxies: kinematics and dynamics — galaxies: spiral — galaxies: structure

1. INTRODUCTION

It is well known that spiral galaxies are not axisymmetric in their global light distribution as seen for example in M101 (NGC 5457) or in NGC 1637 (Sandage 1961). The spatial extent of atomic hydrogen gas, H I, in the outer regions in the two halves of some galaxies was shown to be asymmetric by Baldwin, Lynden-Bell, & Sancisi (1980), who termed such galaxies as *lopsided*. The asymmetry in mass distribution is given by a $\cos\varphi$ distribution, where ϕ is the azimuthal angle in the galactic disk plane. The mapping of global H I profiles of larger samples of galaxies show that nearly 50% of the galaxies show such asymmetry (Richter & Sancisi 1994; Haynes et al. 1998). Recently lopsidedness has also been detected in the old stellar component at smaller radii within the optical image in spiral galaxies via near-IR observations (Block et al. 1994; Rix & Zaritsky 1995) and via *R*-band photometry (Kornreich, Haynes, & Lovelace 1998). For example, 30% of the field spiral galaxies studied show a 20% or larger fractional amplitude for the azimuthal $m = 1$ Fourier component; and the amplitude increases with radius (Rix & Zaritsky 1995; Zaritsky & Rix 1997). Thus the lopsided disk distribution appears to be common in spiral galaxies and is stronger at larger radii.

The physical origin of the lopsided disk distribution is not yet understood, though tidal interactions between galaxies (Beale & Davies 1969) and a satellite galaxy accretion (Walker, Mihos, & Hernquist 1996; Zaritsky & Rix 1997) are strongly indicated as generating mechanisms for the lopsided distribution. For the specific case of the Galaxy, Weinberg (1995) has shown that the tidal interaction between the Galaxy and the LMC causes a global lopsided distortion in the Galaxy halo, which then distorts the galactic disk. Since galaxy interactions are now believed to be extremely common (e.g., Wielen 1990; Schweizer 1999), we assume this to be a general mechanism for creating a lopsided distribution in the halo.

In this paper, we study the dynamics of the response of an axisymmetric galactic disk, perturbed by a lopsided halo potential, and show that the disk self-gravity plays a crucial role in determining the net lopsided distribution in the disk. The self-gravitational potential corresponding to the nonaxisymmetric, self-consistent density response of the disk is calculated and shown to oppose the perturbation potential. The negative disk response decreases the magnitude of the perturbation lopsided potential in a spiral galaxy and also restricts its importance to radii beyond one and a half disk scale lengths—in good agreement with observations. The results are valid irrespective of the mechanism for the origin of the lopsided perturbation.

In an earlier paper (Jog 1997) we had studied the dynamics of orbits in an axisymmetric, exponential disk perturbed by a lopsided halo potential, where it was shown that the maximum of the effective disk density occurs along the maximum of the lopsided potential. It was argued that, qualitatively, this implies that the self-gravitational potential corresponding to this disk response would be anticorrelated with the imposed lopsided halo potential. The aim of this paper is to study this anticorrelation effect quantitatively and to treat the disk response self-consistently.

Since the disk response tends to damp the imposed halo potential, it may seem surprising that the phenomenon of lopsidedness is observed with such a high frequency in spiral galaxies and that the magnitude of the observed disk lopsidedness is fairly high. Note, however, that the halo becomes dynamically more important than the disk at large radii. Thus the damping due to the disk response will be less

important at large radii; therefore, we can expect that the net lopsided distribution would be stronger in the outer regions of disks. Thus we provide a dynamical explanation for the well-known observation that lopsided distribution in disks is stronger at larger radii.

In § 2 the self-gravitational potential corresponding to the nonaxisymmetric disk response is obtained first for a general azimuthal wavenumber m, and then its value is evaluated for the lopsided ($m = 1$) case. A self-consistent calculation yields the net lopsidedness in a galaxy (§ 3), and this is shown to be important only beyond a radius of 1.4 disk scale lengths, in exact agreement with the observations of stellar disks by Rix & Zaritsky (1995). The net reduction in the perturbation potential is obtained, for typical giant spiral galaxies and also for dwarf spiral galaxies, and thus it is checked which galaxies are more likely to display a net lopsided behavior. These results are shown to compare well with the observations of lopsided galaxies. A few general points are discussed in § 4, and the results from this paper are summarized in § 5.

A similar anticorrelation between the disk response and the imposed perturbation potential has been mentioned for the $m = 2$ case by Rix (1996) and by Rix & Zaritsky (1995), though they do not work out the details. The anticorrelation in the surface density response (though not potential) for the closed loop orbits for a general even m Fourier component for a disk of logarithmic potential has been shown by Kuijken (1993). The decrease in ellipticity of the potential due to the disk response to the $m = 2$ perturbation potential has been discussed by Binney (1996). In a future paper, we will study the detailed, self-consistent anticorrelation problem for the $m = 2$ case, analogous to the $m = 1$ case studied here.

2. POTENTIAL CORRESPONDING TO THE DISK RESPONSE

Next, the self-gravitational potential corresponding to the density response of an axisymmetric galactic disk perturbed by a small lopsided halo potential is calculated, using the inversion techniques for the Poisson equation for a thin disk.

2.1. *Density Response in a Lopsided Potential*

First, we summarize the main results from Jog (1997) for the density response of closed loop orbits in an azimuthally symmetric galactic disk perturbed by a lopsided halo potential and their relation to the isophotal shapes in an exponential disk.

The unperturbed potential for the axisymmetric galactic disk ψ_0, at a given radius R is chosen to be a logarithmic potential of the form

$$\psi_0(R) = V_c^2 \ln R \,, \tag{1}$$

where R is measured from the axis of the cylindrical coordinate system. This is applicable for a region of flat rotation, with V_c being the constant rotational velocity. The case of a generalized rotation curve is discussed in § 2.1.1.

The perturbation lopsided halo potential $\psi_{\rm lop}$ is chosen to be nonrotating and equal to

$$\psi_{\rm lop}(R) = V_c^2 \, \epsilon_{\rm lop} \cos \phi \,, \tag{2}$$

where $\epsilon_{\rm lop}$ is a small constant perturbation parameter, and ϕ is the azimuthal angle in the disk plane in the cylindrical coordinate system.

The unperturbed mass surface density, $\mu_{\rm un}$, of the stellar disk is assumed to have an exponential distribution in radius as observed in a typical galactic disk (Freeman 1970):

$$\mu_{\rm un}(R) = \mu_0 \exp\left[-(R/R_{\rm exp})\right] , \tag{3}$$

where μ_0 is the central extrapolated surface density, and $R_{\rm exp}$ is the scale length of the exponential disk. The effective surface density for an exponential disk with perturbed orbits in a lopsided potential is obtained as (Jog 1997):

$$\mu(R, \phi) = \mu_0 \exp\left[-\frac{R}{R_{\rm exp}} \left(1 - \frac{\epsilon_{\rm iso}}{2} \cos \phi\right)\right], \tag{4}$$

where $\epsilon_{\rm iso}$ is the ellipticity of an isophote at R. Further, the following useful relations are obtained (Jog 1997) between $\epsilon_{\rm iso}$; A_1/A_0, the fractional amplitude of the $m = 1$ azimuthal Fourier component of the disk surface brightness; and $\epsilon_{\rm lop}$:

$$\frac{A_1}{A_0} = \frac{\epsilon_{\rm iso}}{2} \frac{R}{R_{\rm exp}} \,; \tag{5}$$

$$\epsilon_{\rm lop} = \frac{A_1/A_0}{2(1/2 + R/R_{\rm exp})} \,. \tag{6}$$

Thus, the change in the surface density, $\mu_{\rm response}$, resulting from the response of the disk to the lopsided potential, is given by subtracting $\mu_{\rm un}$, the unperturbed surface density (eq. [3]) from equation (4). Since $\epsilon_{\rm iso}$ is a small quantity, we obtain:

$$\mu_{\rm response}(R, \phi) = \mu_{\rm un}(R)\left(\frac{R}{R_{\rm exp}} \frac{\epsilon_{\rm iso}}{2} \cos \phi\right) . \tag{7}$$

Using equation (5), this reduces to

$$\mu_{\rm response}(R, \phi) = \mu_{\rm un}(R)\left(\frac{A_1}{A_0} \cos \phi\right) . \tag{8}$$

Thus, the response density is maximum along $\phi = 0°$, along which the lopsided halo potential is also a maximum. This dependence would be true for any self-gravitating, centrally concentrated disk.

2.1.1. *Orbits in a General Rotation Curve*

Recall the results obtained by Jog (1997) for a general power law rotation curve of the form:

$$V = V_c(R/R_0)^{\alpha} \,, \tag{9}$$

where V_c is the circular velocity at R_0, and α is a non-zero small number (< 1) and is the logarithmic slope of the rotation curve. The corresponding unperturbed potential, ψ_0, is:

$$\psi_0(R) = (V_c^2/2\alpha)(R/R_0)^{2\alpha} \,. \tag{10}$$

The perturbation potential in this case is assumed to be

$$\psi_{\rm lop}(R) = V^2 \epsilon_{\rm lop} \cos \phi \,, \tag{11}$$

where V is defined by equation (9). The relation between $\epsilon_{\rm lop}$ and A_1/A_0 in this case is

$$\epsilon_{\rm lop} = \frac{A_1/A_0}{2[(1/2 - \alpha) + (R/R_{\rm exp})(1 - \alpha)]} \,. \tag{12}$$

The response surface density is again given by equation (8).

2.2. *Disk Response Potential: General Nonaxisymmetric Case*

The self-gravitational potential $\psi(R, \phi, z)$ is derived for a general, nonaxisymmetric, thin disk with a surface density $\mu(R, \phi)$, where the galactic cylindrical coordinate system is used. This is obtained by solving the Poisson equation using the inversion technique involving the Hankel transforms of the potential-density pairs. This is a generalization of the method studied earlier for the axisymmetric case by Toomre (1963) (also see Binney & Tremaine [1987]).

For a thin disk, the potential ψ satisfies Laplace's equation everywhere except in the plane of the disk, that is, at $z = 0$. Hence, we first obtain the solution to Laplace's equation. Using the technique of separation of variables, this solution in cylindrical coordinates is given (e.g., Arfken 1970) as follows:

$$\psi(R, \phi, z) = \sum_{m=-\infty}^{\infty} \exp(im\phi) \exp(\pm kz) J_m(kR) , \quad (13)$$

where $J_m(kR)$ is the cylindrical Bessel function of the first kind, of order m. The other linearly independent solution is not considered here since it is proportional to $Y_m(kR)$, the cylindrical Bessel function of the second kind, of order m, which does not remain finite at $R = 0$ and hence is not a physically meaningful solution.

At the plane $z = 0$, the potential gradient is not zero, and the solution for ψ must satisfy the Poisson equation. Define the function

$$\psi_{k,m}(R, \phi, z) \equiv \exp(im\phi) \exp(-k|z|) J_m(kR) . \quad (14)$$

It can be shown that this satisfies the Poisson equation if the corresponding surface density of the thin disk is (Clutton-Brock 1972):

$$\mu_{k,m}(R, \phi) = -\frac{k}{2\pi G} \exp(im\phi) J_m(kR) . \quad (15)$$

Thus, $\psi_{k,m}(R, \phi, z)$ and $\mu_{k,m}(R, \phi)$ constitute a potential-density pair for a nonaxisymmetric thin disk.

Now, assume that a function $S_m(k)$ can be obtained such that the total disk surface density $\mu(R, \phi)$ could be represented as

$$\mu(R, \phi) = \sum_{m=-\infty}^{\infty} \int_0^{\infty} S_m(k) \mu_{k,m}(R, \phi) dk . \quad (16)$$

Using equation (15), this reduces to

$$\mu(R, \phi) = -\frac{1}{2\pi G} \sum_{m=-\infty}^{\infty} \exp(im\phi) \int_0^{\infty} S_m(k) J_m(kR) k dk . \quad (17)$$

Therefore, using the property of the potential-density pairs (eqs. [14] and [15]) and the fact that the Poisson equation is linear, the net potential in the disk can be written as

$$\psi(R, \phi, z) = \sum_{m=-\infty}^{\infty} \exp(im\phi) \times \int_0^{\infty} S_m(k) J_m(kR) \exp(-k|z|) dk . \quad (18)$$

From equation (17) it can be seen that $(-G\mu)$ is the Hankel (or Fourier-Bessel) transform of $(1/2\pi) \sum_{m=-\infty}^{\infty} [\exp(im\phi) S_m(k)]$ (e.g., Arfken 1970). We obtain an expression for the latter in terms of $\mu(R, \phi)$, using the general idea of the inversion of integral transforms:

$$\frac{1}{2\pi} \sum_{m=-\infty}^{\infty} \exp(im\phi) S_m(k) = -\sum_{m'=-\infty}^{\infty} G \int_0^{\infty} J_{m'}(kR) \mu(R, \phi) R dR . \quad (19)$$

Multiplying both sides by $\exp(-im'\phi)$ and integrating over $\phi = 0$ to 2π, we get

$$\delta_{m,m'} \sum_{m=-\infty}^{\infty} S_m(k) = -\sum_{m'=-\infty}^{\infty} G \int_0^{\infty} J_{m'}(kR) R dR \times \int_{\phi=0}^{2\pi} \mu(R, \phi) \exp(-im'\phi) d\phi . \quad (20)$$

Therefore,

$$S_m(k) = -G \int_0^{\infty} J_m(kR) R dR \int_{\phi=0}^{2\pi} \mu(R, \phi) \exp(-im\phi) d\phi . \quad (21)$$

Substituting this in equation (18), we obtain the expression for the nonaxisymmetric potential for the thin disk to be

$$\psi(R, \phi, z) = -G \sum_{m=-\infty}^{\infty} \exp(im\phi) \times \int_0^{\infty} J_m(kR) \exp(-k|z|) dk \times \int_0^{\infty} J_m(kR') R' dR' \times \int_0^{2\pi} \mu(R', \phi') \exp(-im\phi') d\phi' . \quad (22)$$

2.3. *Disk Response Potential: $|m| = 1$ Case*

The general result for the potential for the nonaxisymmetric case (eq. [22]) is applied to the case of the surface density response, μ_{response} (eq. [8]) of an axisymmetric, exponential disk to a lopsided potential. The resulting potential defines the disk response potential, ψ_{response}. Consider the potential in the plane of the disk so that $z = 0$. Since $\mu_{\text{response}}(R', \phi')$ is proportional to $\cos \phi'$, only the values of $m = \pm 1$ need to be kept in the integral over ϕ' on the right-hand side of equation (22), because only these will leave this integral non-zero. Further, since $\cos \phi'$ is an even function of ϕ', and since $J_{-1}(kR) = -J_1(kR)$; the terms for $m = 1$ and $m = -1$ contribute equally to ψ_{response}. On substituting for A_1/A_0 from equation (6), the expression for the response potential, ψ_{response}, is obtained to be:

$$\psi_{\text{response}}(R, \phi) = -2\pi G \mu_0 \cos \phi \int_0^{\infty} J_1(kR) dk \times \int_0^{\infty} J_1(kR') R' \exp\left(-\frac{R'}{R_{\text{exp}}}\right) \times [\epsilon_{\text{lop}}(1 + 2R'/R_{\text{exp}})] dR' . \quad (23)$$

The first integral over R' is solved, using relation (6.623.1) from Gradshteyn & Ryzhik (1980), to be

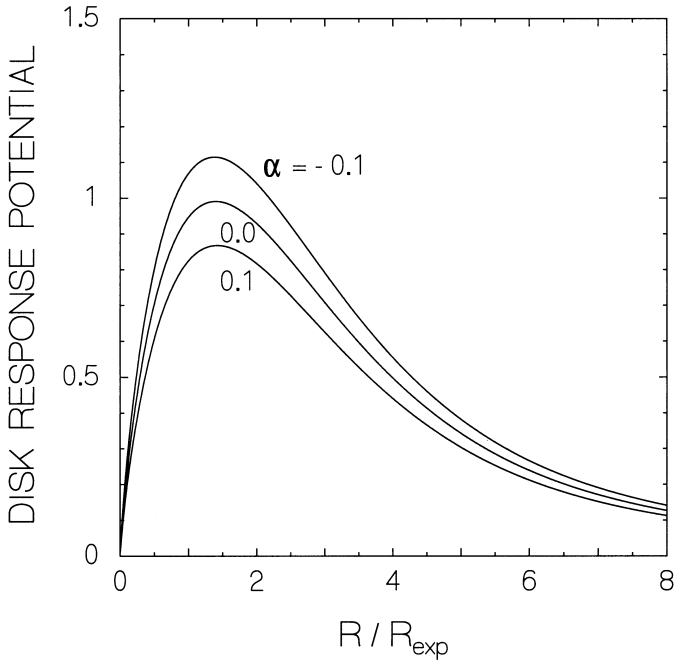

FIG. 1.—Magnitude of the dimensionless disk response potential γ vs. dimensionless radius $R/R_{\rm exp}$ for different logarithmic slopes (α) of the rotation curve; $\alpha = 0$, $\alpha > 0$, $\alpha < 0$ denote flat, increasing, and decreasing rotation curves, respectively. The maximum occurs at a radius of 1.4 disk scale lengths, and this radius is nearly independent of the slope of the rotation curve.

$$\int_0^\infty J_1(kR')R' \exp\left(-\frac{R'}{R_{\rm exp}}\right)dR' = \frac{k}{(k^2 + 1/R_{\rm exp}^2)^{3/2}} . \quad (24)$$

The second integral over R' is solved using relation (6.623.2) from Gradshteyn & Ryzhik (1980), to be

$$\int_0^\infty J_1(kR')R'^2 \exp\left(-\frac{R'}{R_{\rm exp}}\right)dR' = \frac{3k}{R_{\rm exp}(k^2 + 1/R_{\rm exp}^2)^{5/2}} . \quad (25)$$

On substituting equations (24) and (25) in equation (23), it reduces to

$$\begin{aligned}\psi_{\rm response}(R, \phi) = & -\left\{(2\pi G\mu_0 R_{\rm exp})\epsilon_{\rm lop} \cos\phi\left(\frac{R}{R_{\rm exp}}\right)\right. \\ & \left.\times \int_0^\infty \frac{J_1(x)xdx}{[x^2 + (R/R_{\rm exp})^2]^{(3/2)}}\right\} \\ & -\left\{(2\pi G\mu_0 R_{\rm exp})\epsilon_{\rm lop} \cos\phi\, 6\left(\frac{R}{R_{\rm exp}}\right)^3\right. \\ & \left.\times \int_0^\infty \frac{J_1(x)xdx}{[x^2 + (R/R_{\rm exp})^2]^{(5/2)}}\right\} . \end{aligned} \quad (26)$$

Note that $\psi_{\rm response}$ has a sign opposite to the perturbation potential $\psi_{\rm lop}$ (eq. [2]), thus the disk response potential is negative, and in the linear regime studied here it has a magnitude proportional to $\epsilon_{\rm lop}$, the perturbation parameter in $\psi_{\rm lop}$, and cos ϕ. A similar negative disk response would be obtained for any self-gravitating disk. $\psi_{\rm response}$ denotes the disk response potential induced by the imposed lopsided potential alone. Here we have not taken account of further effect on the disk of this response potential, whereas in § 3.1 we obtain the net disk response self-consistently.

Next, define a dimensionless quantity, η, to be the ratio of the magnitude of the response potential (eq. [26]) and the lopsided potential (eq. [2]):

$$\eta \equiv |\psi_{\rm response}|/\psi_{\rm lop} . \quad (27)$$

Note that η is independent of the strength of the lopsided perturbation, $\epsilon_{\rm lop}$, and at a given radius it depends linearly on $\mu_0 R_{\rm exp}/V_c^2$. This property of η will be used in obtaining the self-consistent disk response in § 3.1.

For a general rotation curve, the relation between A_1/A_0 and $\epsilon_{\rm lop}$ is given by equation (12); on substituting this into equation (22), a result for $\psi_{\rm response}$ is obtained that is similar to equation (26) with the same integrals over x, except that now the first and the second terms on the right-hand side of equation (26) are multiplied by $(1 - 2\alpha)$ and $(1 - \alpha)$ respectively. Using these, an expression similar to η (eq. [27]) is obtained for the general case.

The integrals in equation (26) are solved numerically using the standard numerical procedure for calculating J_1, the cylindrical Bessel function of the first kind, of order 1 (Press et al. 1986).[1] The radial variation in the magnitude of the disk response potential can be illustrated in terms of a dimensionless response potential, γ, defined as η (eq. [27]) times a constant $V_c^2/2\pi G\mu_0 R_{\rm exp}$:

$$\gamma = \frac{|\psi_{\rm response}|}{\psi_{\rm lop}} \frac{V_c^2}{2\pi G\mu_0 R_{\rm exp}} . \quad (28)$$

In Figure 1, γ vs $R/R_{\rm exp}$ is plotted for a flat rotation curve with the slope $\alpha = 0$ and also for an increasing and a decreasing rotation curve with $\alpha = 0.1$ and -0.1 respectively. The maximum occurs at radii of 1.38, 1.40, and 1.42 $R_{\rm exp}$, respectively, for the slopes $\alpha = -0.1$, 0.0, and 0.1; that is, at a typical radius of 1.4 disk scale lengths. This value is robust and is nearly independent of the slope of the rotation curve. Even for slopes of $\alpha = -0.2$ and 0.2 (not shown in the figure), which occur less often, the maximum occurs at a radius of $1.37R_{\rm exp}$ and $1.45R_{\rm exp}$, respectively. The observational consequences of this result will be discussed in § 3.2. The value of γ is lower for the disk with an increasing rotation curve.

3. RESULTS

3.1. *Net Lopsided Potential: Self-consistent Calculation*

In this section, we obtain the net nonaxisymmetric (lopsided) potential, $\psi_{\rm net}$, in the disk plane using a self-consistent treatment. In § 2.3 the results were presented for the potential corresponding to the disk response (eq. [26]) to the perturbation lopsided potential (eq. [2]) alone. Clearly, a particle in the disk will be affected by both the imposed potential and the potential corresponding to the stellar disk response to it. However, the net lopsided potential $\psi_{\rm net}$ cannot be obtained by simply adding these two linearly. Instead, for a self-consistent treatment, $\psi_{\rm net}$ must be defined as follows:

$$\psi_{\rm net} = \psi_{\rm lop} + \psi' , \quad (29)$$

[1] If the first integral is solved analytically using relation (6.565.8) from Gradshteyn & Ryzhik (1980), it results in the magnitude of the $\psi_{\rm response}$ increasing monotonically with radius—which is unphysical since the response of an exponential disk should fall off at large radii. This error comes about because the range of exponents for the validity of the above relation are given incorrectly in Gradshteyn & Ryzhik (1980); see Watson (1944), p. 434 for the correct range.

where ψ' is the self-gravitational potential corresponding to the net, self-consistent change in the disk surface density, $\mu_{\text{response}'}$, which is obtained as a response to the net potential, ψ_{net}. This self-consistent approach is similar to the treatment of the stellar disk response to an imposed cloud potential studied by Julian & Toomre (1966).

The above equation can be solved in a straightforward way because even though ψ' or $\mu_{\text{response}'}$, are not known a priori, both would nonetheless be proportional to cos ϕ (§ 2.3). Hence ψ' would have a form similar to equation (26), and it would oppose ψ_{net}. In particular, the ratio of ψ' to ψ_{net} would be given identically by the ratio $-\eta$ (eq. [27]), which was obtained for the disk response to the imposed potential alone. Thus we get:

$$\psi' = -\psi_{\text{net}}\,\eta\ . \tag{30}$$

On substituting this into equation (29), we get:

$$\psi_{\text{net}} = \frac{\psi_{\text{lop}}}{1+\eta} = \psi_{\text{lop}}\,\delta\ , \tag{31}$$

where $\delta(\leq 1)$ is defined to be the reduction factor by which the magnitude of ψ_{lop} is reduced due to the self-consistent, negative disk response. Note that $\delta = 1$ corresponds to no reduction effect. Since η is a positive definite quantity (see eq. [27]), therefore, the magnitude of the net lopsided potential in the plane of the galactic disk is always smaller than that of the perturbation lopsided halo potential. Check that for $\eta = 0$, corresponding to zero disk response, $\psi_{\text{net}} = \psi_{\text{lop}}$ is obtained, as expected physically. Note that the net disk response potential, ψ', is smaller in magnitude by a factor $(1+\eta)$ than the disk response to the imposed potential alone (see eq. [27]).

From equation (31), the reduction factor, δ, is defined as

$$\delta \equiv \frac{1}{1+\eta}\ , \tag{32}$$

where η is defined by equation (27). Thus η and hence the reduction factor δ at a given radius R/R_{exp} are independent of the strength of the lopsided perturbation ϵ_{lop}, and δ depends inversely on $\mu_0 R_{\text{exp}}/V_c^2$ (see § 2.3). Similarly, using η for the general rotation curve ($\alpha \neq 0$; see § 2.3), a similar expression for δ is obtained for the general case. Recall from Figure 1 that η times a constant $(= V_c^2/2\pi G\mu_0 R_{\text{exp}})$ decreases monotonically with radius beyond 1.4 disk scale lengths, hence δ increases steadily beyond this radius. The actual values of δ are presented in § 3.3.

In analogy with the definition of ψ_{lop}, we now define ψ_{net} in terms of a small perturbation parameter ϵ_{net} as follows:

$$\psi_{\text{net}} \equiv V_c^2\,\epsilon_{\text{net}}\cos\,\phi\ . \tag{33}$$

Substituting this, and equation (2) for ψ_{lop}, into equation (31), we obtain:

$$\epsilon_{\text{net}} = \epsilon_{\text{lop}}\,\delta\ . \tag{34}$$

Thus, the parameter ϵ_{net}, denoting the strength of the net lopsided potential in the galactic disk, is reduced in comparison with ϵ_{lop}, the parameter denoting the halo lopsided potential, by the reduction factor δ.

In the self-consistent approach used here, the force equation and the continuity equation would involve ψ_{net} (eq. [29]). Hence, the surface density change obtained from these two equations for the halo-alone case earlier (eq. [6]) would now be modified by taking account of the negative disk response, and can be shown to be

$$\epsilon_{\text{net}} = \frac{A_1/A_0}{2(1/2 + R/R_{\text{exp}})}\ . \tag{35}$$

Thus, the observations of A_1/A_0, the fractional amplitude of the $m = 1$ azimuthal Fourier component of the surface brightness, will measure ϵ_{net}. Formally, the net density response, $\mu_{\text{response}'}$, will still be given by equation (8), except that A_1/A_0 is now defined by equation (35) for the self-consistent treatment. Similarly, for a general rotation curve, ϵ_{net} will now be equal to the right-hand side of equation (12).

The net observed lopsided amplitude in the disk (A_1/A_0) may be used as a diagnostic to obtain an estimate of the true halo lopsidedness ϵ_{lop} (see eqs. [35] and [34]) if the value of δ is known. The typical minimum value of δ is $\sim$0.5–0.7 (§ 3.3), say $\sim$0.6. Thus the values of the true lopsided parameter ϵ_{lop} are obtained to be $\sim$0.03–0.05 for the typical observed values of $A_1/A_0 = 0.14$–0.20 (Rix & Zaritsky 1995). Note that these are higher by a factor $1/\delta \sim 1.6$ compared with the values of ϵ_{lop} obtained using equation (6) by Jog (1997). That is, for a given observed A_1/A_0, the magnitude of the true halo lopsidedness required to produce this despite the negative disk response is higher, by a factor of $\sim$1.6, compared with a disk without self-gravity.

The kinematical study of lopsided distribution in individual galaxies (e.g., Schoenmakers, Franx, & de Zeeuw 1997) also yields a value of the lopsided halo potential. The results in the present paper show that the true halo lopsidedness in those cases would be higher by a factor of $\sim$1.6 than the value deduced by the authors.

3.2. *Radial Dependence: Comparison with Observations*

We study the radial dependence of the net lopsided distribution and show that the results compare well with observations of lopsided galaxies.

The observed measure of disk lopsidedness is A_1/A_0, which is shown to be proportional to ϵ_{net} (eq. [35]), hence it is proportional to ϵ_{lop} and the reduction factor, δ (eq. [34]). As shown in § 3.1, δ increases monotonically beyond a radius of 1.4 disk scale lengths. The values of ϵ_{lop} are not calculated here, but it is either a constant, as assumed here for simplicity (eq. [2]), or more likely, it increases with radius if it is of tidal origin. Thus, both ϵ_{net} and A_1/A_0 increase monotonically beyond the radius of 1.4 disk scale lengths for a constant ϵ_{lop}. This radial dependence is robust and is independent of the slope of the rotation curve.

This radial dependence of A_1/A_0 is valid even if ϵ_{lop} were to increase with radius, because δ is independent of ϵ_{lop} (§ 3.1) and has a minimum at $1.4R_{\text{exp}}$ as shown above. Hence, in this case, the quantitative increase in ϵ_{net} beyond this radius would be even higher. Only a future systematic study via numerical simulations can give the quantitative values of ϵ_{lop} and its radial variation.

Thus we show that the net lopsided distribution in a galactic disk would only be detectable at large radii, beyond a radius of 1.4 disk scale lengths, and its amplitude would increase with radius beyond that. This is in exact agreement with the observations of stellar disks made by Rix & Zaritsky (1995), who found that the values of A_1/A_0 are small over 1–2 disk scale lengths and increase beyond these radii. They give the value at a radius of $2.5R_{\text{exp}}$ as an indica-

tor of the lopsidedness, since that is the highest radius at which the near-IR measurement of the average surface density can be done. Zaritsky & Rix (1997) have confirmed this radial dependence for a larger sample of galaxies, and they give an average value of A_1/A_0 between 1.5 and $2.5R_{exp}$ as an indicator of lopsidedness in a galactic disk.

The results for the dynamics of orbits (§ 2.1) are equally applicable for the gas in the disk, as shown by Jog (1997). The gas would also experience the net lopsided potential (eq. [31]) in the disk plane. The above radial dependence of δ therefore provides a natural explanation as to why lopsided distribution in the atomic hydrogen gas is observed mainly in the outer disk (e.g., Baldwin et al. 1980). We further predict that the amplitude of lopsidedness would be stronger in the H I gas than in the stars, since H I extends much farther out than the optical (stellar) disk, typically up to 1.5 Holmberg radii (Giovanelli & Haynes 1988). In order to check this, we need to have quantitative measurements of asymmetry in H I and its radial dependence analogous to the A_1/A_0 values for the stellar disks. This would also allow one to estimate the lopsided halo distribution (see § 3.1) in the outer disk.

3.3. *Reduction Factor*

The value of the reduction or scaling factor δ (defined by eq. [31]) is calculated numerically and its variation is studied with the galaxy morphological type, the galaxy size, and radius in the galactic disk. The aim is to see which galaxies have a large δ and hence are most likely to display a net lopsided disk distribution. As shown in § 3.1, the value of δ depends inversely on $\mu_0 R_{exp}/V_c^2$. The typical values of δ are obtained separately for the classical large or giant spiral galaxies (as defined, for example, by Mihalas & Binney 1981) and for the dwarf galaxies. The parameters used here pertain to the high surface brightness galaxies. In this paper, we do not treat the case of the low surface brightness galaxies (Bothun, Impey & McGaugh 1997).

3.3.1. *Giant Spiral Galaxies*

First consider the giant spirals. The value of μ_0 can be obtained by combining the observed central extrapolated surface intensity and the mass-to-light ratio for the disk. The value of the central surface intensity is known to be remarkably constant with galaxy type for the giant spirals (Freeman 1970). This has been confirmed for a much larger sample by Van der Kruit (1987), who has also shown that this is not the result of observational selection effects. Since the mass to light ratio is known to be constant to within a factor of 2, Van der Kruit (1987) obtains the typical central surface density μ_0 to be $=450\ M_\odot\ pc^{-2}$.

The other two parameters, R_{exp} and V_c, show a substantial variation with morphological type and further with size for a given type. The values of the maximum rotation velocity V_c lie in the range 200–300 km s^{-1} (Binney & Tremaine 1987). In fact, V_c decreases with type, with the median values for Sa, Sb, and Sc type galaxies being equal to 299, 222, and 175 km s^{-1}, respectively (Rubin et al. 1985). These agree with the values of V_c we calculated for the median of the sample from Roberts & Haynes (1994). Hence, we consider V_c equal to 200, 250, and 300 km s^{-1} as three typical values to span the range of V_c for typical giant spiral galaxies.

The exponential disk scale length, R_{exp}, shows a variation from 1 to 5 kpc, with no clear dependence on type; and the larger galaxies show a larger scale length (Freeman 1970; Van der Kruit 1987). The typical representative scale length is 3 kpc (Binney & Tremaine 1987); therefore, $R_{exp} = 3$ kpc was used. Note that we could equally have taken a typical $V_c = 250$ km s^{-1} and taken the range of 1–5 kpc for R_{exp} to effectively span the entire parameter space.

Figure 2 contains a plot of the reduction factor δ, the factor by which the halo lopsided potential is reduced due to the negative response of the disk (eq. [32]), versus R/R_{exp} for $R_{exp} = 3$ kpc, and for the values of $V_c = 200$, 250, and 300 km s^{-1} for a flat rotation curve. Note that in each case δ is a minimum at $1.4R_{exp}$ and increases thereafter, as explained in § 3.1. The typical minimum value of δ lies in the range 0.5–0.7, and at a given radius, δ is larger for galaxies with a larger value of V_c.

It is interesting to obtain the effect of negative disk response in the case of the Milky Way. We assume a flat rotation curve with $V_c = 220$ km s^{-1}, $R_{exp} = 3.5$ kpc (Binney & Tremaine 1987); and $\mu_0 = 450\ M_\odot\ pc^{-2}$ as discussed above for the giant galaxies; and obtain the plot of δ versus R/R_{exp} as given in Figure 3. Note that this is similar to the plot for a typical giant spiral galaxy (see Fig. 2), and that the minimum value of δ is 0.53, and it occurs at a radius of $1.4R_{exp}$. Thus, if the halo of our Galaxy has a lopsided distortion, say due to perturbation via galaxy interaction, the disk response would reduce this potential by a factor of more than 0.53. The net disk lopsidedness would only be important beyond a radius of $1.4R_{exp}$ (see § 3.2), that is, beyond 4.9 kpc.

3.3.2. *Dwarf Spiral Galaxies*

The spiral galaxies of type Scd and later (Sd–Im) are physically different in that they are smaller, with a smaller disk scale length $R_{exp} \leq 1$ kpc (Freeman 1970), and are less luminous. These are far more numerous than the giant spirals (e.g., Mihalas & Binney 1981), hence it is important

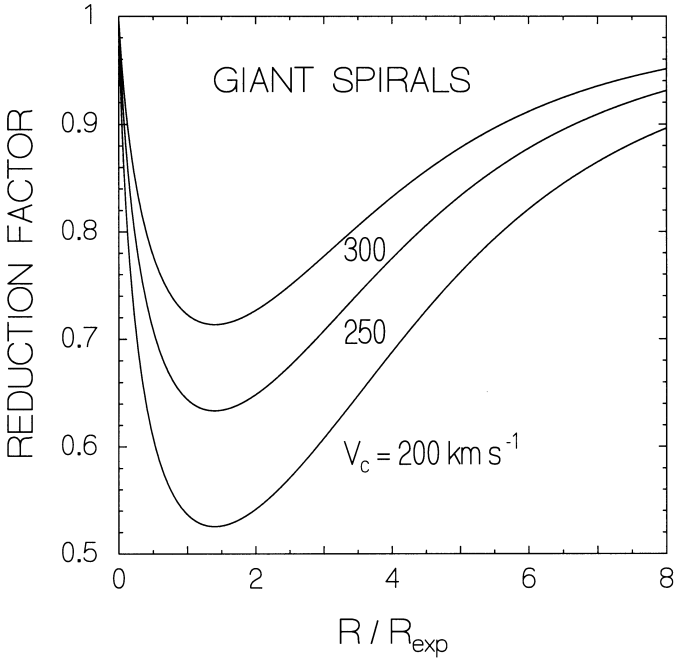

FIG. 2.—Reduction factor δ for the lopsided potential due to the negative disk response vs. radius R/R_{exp}, for giant spiral galaxies, with a flat rotation curve with velocity $V_c = 200$, 250, and 300 km s^{-1}, and $R_{exp} = 3$ kpc. The minimum reduction factor lies in the range of 0.5–0.7; for each case it occurs at $R/R_{exp} = 1.4$, and δ increases steadily beyond this radius.

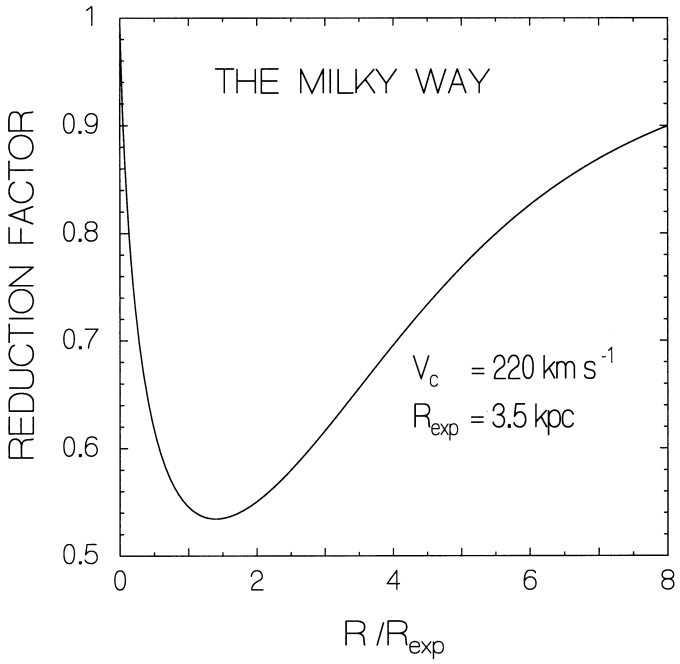

FIG. 3.—Reduction factor δ vs. radius R/R_{exp}, for the Milky Way, with a flat rotation curve with velocity $V_c = 220$ km s^{-1} and $R_{exp} = 3.5$ kpc. The minimum reduction factor is 0.53, similar to that for typical giant spiral galaxies (see Fig. 2).

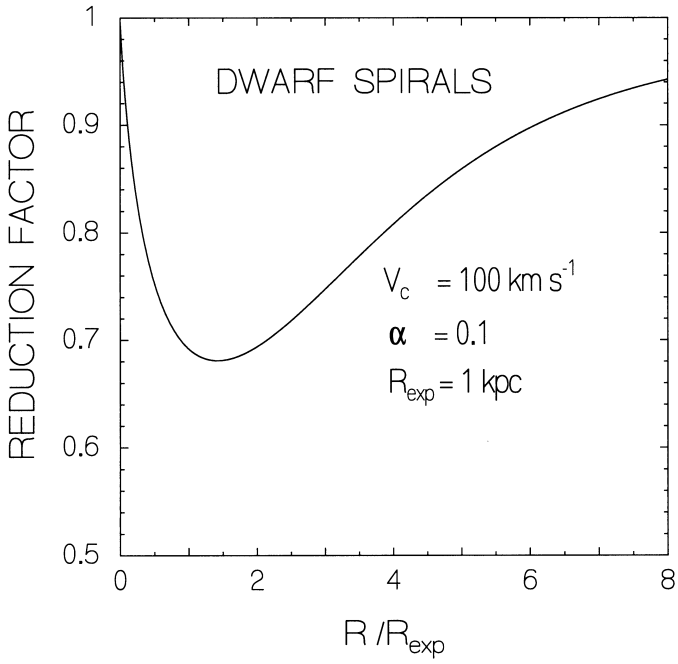

FIG. 4.—Reduction factor δ vs. radius R/R_{exp}, for dwarf spiral galaxies, with $V_c = 100$ km s^{-1}, and an increasing rotation curve with a slope $\alpha = 0.1$, and $R_{exp} = 1$ kpc. The minimum reduction factor is 0.68, and it occurs at $R/R_{exp} = 1.42$, similar to that for typical giant spiral galaxies (see Fig. 2).

to obtain δ for them. Van der Kruit (1987) calls these morphological dwarfs and obtains for them a smaller $\mu_0 = 200$ $M_\odot$ pc^{-2} and $R_{exp} = 1$ kpc; here these values have been used to obtain the reduction factor for the dwarfs. Roberts & Haynes (1994) have also stressed that these galaxies form a different class, and from their H I data, we obtain the median value of $V_c = 100$ km s^{-1} for these galaxies. The dwarf galaxies typically show rising rotation curves, and for this velocity the typical observed value of α—the slope of the rotation curve (eq. [9])—is 0.1 (Casertano & Van Gorkom 1991). In Figure 4 the reduction factor δ is plotted for the general case of $\alpha = 0.1$ (see § 3.1) versus R/R_{exp} for $\mu_0 = 200$ $M_\odot$ pc^{-2}, $R_{exp} = 1$ kpc, and $V_c = 100$ km s^{-1}. The minimum reduction factor of 0.68 and also the radius $= 1.42R_{exp}$ at which it occurs, are similar to those for the giant spiral galaxies (see Fig. 2).

3.3.3. *Comparison with Observations*

At a given radius, δ depends inversely on $\mu_0 R_{exp}/V_c^2$ (see eq. [32]), and when this term is smaller, δ is closer to 1, indicating less reduction (see § 3.1). Thus, galaxies with a large value of V_c and small disk scale length R_{exp} will have a higher value of δ and hence show a higher net disk lopsidedness (eq. [34]). This agrees well with the observations of a prototypical lopsided galaxy, such as NGC 2841 with a small $R_{exp} = 2.5$ kpc (e.g., Casertano & Van Gorkom 1991); and also for the strongly lopsided galaxies in the sample by Rix & Zaritsky (1995). We calculated R_{exp} using the information on angular sizes in Rix & Zaritsky (1995), and the spatial distances in Zaritsky & Rix (1997), and found that all the six out of the 18 galaxies in the Rix & Zaritsky (1995) sample showing a significant net disk lopsidedness ($A_1/A_0 \geq 0.2$), have small disk scale lengths; in fact, three of these have values of $R_{exp} < 2$ kpc.

Further, the weak dependence of δ on galaxy type and size (Figs. 2–4) means that, in general, whether a particular type of galaxy is more likely to show net lopsidedness is decided not only by the reduction factor but mainly by the magnitude of the initial lopsided potential ψ_{lop} (see eq. [34]). Since the halo is more dominant in late-type giant spirals and in the dwarf galaxies (e.g., Broeils 1992), these will have a stronger halo lopsidedness and hence are more likely to display a net disk lopsided distribution. This is in agreement with the observations that a large fraction of late-type spirals and dwarfs display lopsidedness.

Alternatively, for the dwarf galaxies, the kinematical model of long-term maintenance of the pattern in the large halo core (Levine & Sparke 1998) may be applicable. In the dwarfs, the center of the outer parts is often shifted compared with that of the central parts (e.g., the model by Levine & Sparke 1998); however, this does not describe the distribution in the giant lopsided spirals, where the center is common but a variation in density distribution along the orbits is deduced from the H I velocity fields (Binney & Merrifield 1998).

4. DISCUSSION

A few general points regarding this study are given below:

1. The origin of the halo lopsided perturbation is most likely of galactic tidal origin (§ 1). We propose that such perturbations of the halo would be long-lived, since the halo is collisionless and is supported by random motion, hence the relaxation time would be much larger than the dynamical timescale—this will be studied in a future paper. Thus, the effects of tidal interaction may be retained in terms of the halo distortion and hence disk lopsidedness long after

the galactic tidal encounter. Consequently, the resulting lopsided galaxy may not even have a close companion at the present epoch. This may explain why a large fraction of the sample studied by Zaritsky & Rix (1997), as well as such galaxies as M101 or NGC 628, which do not appear to have nearby companions at the present epoch, can still display a lopsided distribution. In fact, Zaritsky & Rix (1997) mention a long-term survival of lopsidedness after the encounter as a possible reason for this observation.

2. The perturbation is assumed to be due to halo, hence V_c^2 (eq. [2]) is assumed to be entirely due to the halo. This is strictly correct at large radii ($> 4R_{\rm exp}$), and the halo may be the dominant contributor to the rotation even at 2–3 $R_{\rm exp}$ (Broeils 1992). At smaller radii, the halo contribution to the rotation is smaller, however, taking account of this will only decrease the magnitude of $\psi_{\rm lop}$ and $\psi_{\rm net}$ without affecting the radial variation in δ.

3. It is interesting that for the observed range of the parameters $R_{\rm exp}$, μ_0, and V_c for typical galaxies, the resulting reduction factor is ≥ 0.5–0.7. That is, in real galaxies, the negative disk response due to the disk self-gravity cannot be ignored; hence, the disk cannot be treated as a collection of massless test particles.

5. CONCLUSIONS

We have studied the self-consistent response of an axisymmetric, exponential galactic disk perturbed by a constant lopsided halo potential. The main results from this paper are:

1. The self-gravitational potential of the non-axisymmetric disk response to the perturbation lopsided potential is obtained, by inversion of Poisson equation for a thin disk using the Hankel transforms of the potential-density pairs. The result is obtained first for a general azimuthal wavenumber m and then applied to the lopsided case ($m = 1$). The response potential in the disk plane is shown to oppose the perturbation halo potential.

2. From a self-consistent calculation, the magnitude of the net lopsided potential is shown to be always smaller than the magnitude of the imposed lopsided potential. Further, the net lopsided distribution in the disk is shown to be important only beyond a radius of 1.4 disk scale lengths, and its magnitude increases with radius, indicating the increasing dynamical importance of the halo over the disk at larger radii. This is a robust dynamical result and is independent of the logarithmic slope of the rotation curve.

3. This result agrees well with the observations of radial dependence of lopsidedness of stellar disks by Rix & Zaritsky (1995). It also provides a natural explanation as to why lopsided distribution in the atomic hydrogen gas is observed mainly in the outer disk. In the Galaxy, the disk lopsidedness is predicted to be important only beyond 5 kpc.

4. The negative disk response reduces the magnitude of the perturbation potential by a reduction factor δ that is independent of the strength of the perturbation potential. The typical minimum value of δ is ~ 0.5–0.7 and is insensitive to the galaxy morphological type and size. Thus, in real galaxies, the reduction in perturbation potential due to negative disk response is always significant.

5. Using the typical observed lopsided amplitude in the disk (A_1/A_0) as a diagnostic, and the calculated value of δ, the estimated typical, true halo lopsidedness parameter $\epsilon_{\rm lop}$ is ~ 0.03–0.05.

It would be useful to have quantitative measurements of asymmetry in H I analogous to the A_1/A_0 values for the stellar disks, since it would enable us to estimate the lopsided halo distribution in the outer disk.

I would like to thank the anonymous referee and Monica Valluri for useful comments on the manuscript.

REFERENCES

Arfken, G. 1970, Mathematical Methods for Physicists (2d ed.; New York: Academic)
Baldwin, J. E., Lynden-Bell, D., & Sancisi, R. 1980, MNRAS, 193, 313
Beale, J. S., & Davies, R. D. 1969, Nature, 221, 531
Binney, J. 1996, in IAU Symp. 169, Unsolved Problems of the Milky Way, ed. L. Blitz & P. Teuben (Dordrecht: Kluwer), 1
Binney, J. & Merrifield, M. 1998, Galactic Astronomy (Princeton: Princeton Univ. Press)
Binney, J., & Tremaine, S. 1987, Galactic Dynamics (Princeton: Princeton Univ. Press)
Block, D. L., Bertin, G., Stockton, A., Grosbol, P., Moorwood, A. F. M., & Peletier, R. F. 1994, A&A, 288, 365
Bothun, G., Impey, C., & McGaugh, S. 1997, PASP, 109, 745
Broeils, A. H. 1992, Ph.D. thesis, Groningen Univ.
Casertano, S., & Van Gorkom, J. 1991, AJ, 101, 1231
Clutton-Brock, M. 1972, Ap&SS, 16, 101
Freeman, K. C. 1970, ApJ, 160, 811
Giovanelli, R., & Haynes, M. P. 1988, in Galactic and Extragalactic Radio Astronomy, ed. G. L. Verschuur & K. I. Kellermann (2d ed.; New York: Springer), 522
Gradshteyn, I. S., & Ryzhik, I. M. 1980, Tables of Integrals, Series, and Products (New York: Academic)
Haynes, M. P., Hogg, D. E., Maddalena, R. J., Roberts, M. S., & van Zee, L. 1998, AJ, 115, 62
Jog, C. J. 1997, ApJ, 488, 642
Julian, W. H., & Toomre, A. 1966, ApJ, 146, 810
Kornreich, D. A., Haynes, M. P., & Lovelace, R. V. E. 1998, AJ, 116, 2154
Kuijken, K. 1993, ApJ, 409, 68
Levine, S. E., & Sparke, L. S. 1998, ApJ, 496, L13
Mihalas, D., & Binney, J. J. 1981, Galactic Astronomy (San Francisco: Freeman) chap. 5
Press, W. H., Flannery, B. P., Teukolsky, S. A., & Vetterling, W. T. 1986, Numerical Recipes (Cambridge: Cambridge Univ. Press), chap. 6
Richter, O.-G., & Sancisi, R. 1994, A&A, 290, L9
Rix, H.-W. 1996, in IAU Symp. 169, Unsolved Problems of the Milky Way, ed. L. Blitz & P. Teuben (Dordrecht: Kluwer), 23
Rix, H.-W., & Zaritsky, D. 1995, ApJ, 447, 82
Roberts, M. S., & Haynes, M. P. 1994, ARA&A, 32, 115
Rubin, V. C., Burstein, D., Ford, W. K., & Thonnard, N. 1985, ApJ, 289, 81
Sandage, A. 1961, The Hubble Atlas of Galaxies (Washington, DC: Carnegie Inst. Washington)
Schoenmakers, R. H. M., Franx, M., & de Zeeuw, P. T. 1997, MNRAS, 292, 349
Schweizer, F. 1999, in IAU Symp. 186, Galaxy Interactions at Low and High Redshift, ed. J. Barnes & D. B. Sanders (Dordrecht: Kluwer), in press
Toomre, A. 1963, ApJ, 138, 385
Van der Kruit, P. C. 1987, A&A, 173, 59
Walker, I. R., Mihos, J. C., & Hernquist, L. 1996, ApJ, 460, 121
Watson, G. N. 1944, A Treatise on the Theory of Bessel Functions (2d ed.; Cambridge: Cambridge Univ. Press), 434
Weinberg, M. D. 1995, ApJ, 455, L31
Wielen, R. 1990, Dynamics and Interactions of Galaxies (Berlin: Springer)
Zaritsky, D., & Rix, H.-W. 1997, ApJ, 477, 118